

Dynamic mechanisms for apparent slip on hydrophobic surfaces

Eric Lauga & Michael P. Brenner

Division of Engineering and Applied Sciences,
Harvard University,
29 Oxford Street, Cambridge, MA 02138.

March 3, 2019

Abstract

Recent experiments (Zhu & Granick, *Phys. Rev. Lett.* **87** 096105 (2001)) have measured a large shear dependent fluid slip at partially wetting fluid-solid surfaces. We present a mechanical model for such slip, motivated by the recent observations of stable nanobubbles on hydrophobic surfaces. The model considers the response of nanobubbles to change in hydrodynamic pressure. Both the compression and diffusion of gas in the bubble decrease the viscous force, thereby creating an apparent shear dependent slip. The model reproduces the major features of the experimental measurements.

The validity of the no-slip boundary condition is at the center of our current understanding of fluid mechanics. It remains however an assumption whose microscopic validity has been widely debated [1]. The widespread acceptance of the no-slip condition is based on a historical record of outstanding agreement between experiment and theories. It is commonly agreed [2, 3, 4] that the no-slip condition results from inevitable microscopic roughness, which causes enough viscous dissipation to effectively bring the fluid to rest near the surface. Remarkably, this explanation is independent of the nature of the solid and the liquid, contrary to ideas first proposed by Girard (see [1]).

The development of small devices has prompted a reexamination of fluid slip on length scales of nanometers and microns, both experimentally [5, 6, 9, 7, 10, 11, 8, 4, 12] and theoretically [13, 14, 15, 16, 17]. The degree of slip is quantified by a slip length $\lambda = U_s/\dot{S}$, where U_s is the slip velocity and \dot{S} is the liquid strain rate evaluated at the surface; equivalently, λ is the distance below the solid surface where the velocity extrapolates to zero linearly [19]. In experiments, slip is usually found when the liquid partially wets the solid surface; measured slip lengths span four orders of magnitude, from liquid mean free paths to microns, and are usually shear-dependent in squeeze flow experiments, with λ an increasing function of \dot{S} . In particular, Zhu & Granick [8] report squeeze flow experiments, in which two crossed cylinders oscillate about a fixed average distance. By measuring the viscous resistance, Zhu & Granick extracted the slip length over a wide range of oscillation amplitudes. These experiments lead to the largest shear-dependent slip lengths yet ($\sim 2 \mu\text{m}$).

The origin of this large shear dependent slip is heretofore mysterious. Nanobubbles have recently been observed on hydrophobic surfaces, using atomic force microscopy, with typical thickness $h \sim 10 \text{ nm}$, typical radius $R \sim 100$

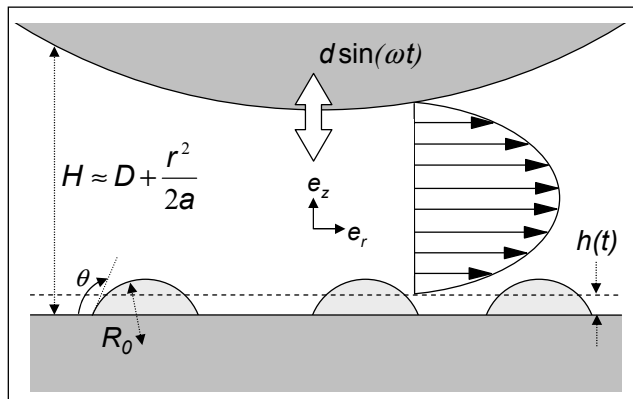


Figure 1: Typical squeeze flow experiment: a solid sphere of radius a is oscillated in a liquid at a distance $D \ll a$ of a smooth solid surface with amplitude $d \ll D$ and frequency ω . The surface is covered by microscopic gas bubbles of contact angle θ and radius of curvature R_0 . The set of bubbles is approximated by a gas layer of time evolving thickness $h(t)$.

nm and high surface coverage [20, 21, 22]. Although the origin of these bubbles remains unclear, they have been often invoked as a possible origin of the so-called hydrophobic attraction [23, 24, 25, 27, 26, 28, 29, 30, 31] and their existence points to a possible picture for such large slip, as pointed out by de Gennes [32].

It is well known that there *is* slip at a solid-gas interface, and therefore it is natural to wonder whether the existence of such a gas layer at the solid surface is sufficient to explain the experiments. When a fluid of viscosity η_1 adjoins a layer of fluid of thickness h with smaller viscosity η_2 , the discontinuous strain rate at the fluid-fluid interface results in an apparent slip with $\lambda = h(\eta_1/\eta_2 - 1)$ [33]. Choosing $\eta_1/\eta_2 = 50$ appropriate for a gas-water interface, leads to slip lengths as large as 500 nm. This estimate is however independent of the interfacial shear and therefore unable to explain the shear dependence of the slip lengths reported in experiments.

In this Letter, we will examine the *dynamic* response of the nanobubbles, which we will assume to exist on hydrophobic surfaces, to an imposed oscillatory shear. In an oscillatory squeeze flow experiment [8], we argue that the pressure fluctuations in the fluid cause the nanobubbles to act as a “leaking mattress”, with both compression and dilation of the gas in the bubble, as well as diffusion of gas into (and out of) the bubble. Both of these effects decrease the force required to move the plates, and hence create an apparent slip. Our calculations indicate that the magnitude and shear dependence of this slip is consistent with the observations of Zhu & Granick. We find quantitative agreement with two fitting parameters, the area fraction and average radius of the nanobubbles.

A typical oscillatory squeeze flow experiment (with notation defined) is shown in Figure 1. The peak lubrication force opposing the motion of the oscillating sphere is given by

$$F_{lub} = f^* \frac{6\pi\eta a^2}{D} d\omega. \quad (1)$$

Any deviation $f^* < 1$ is interpreted as fluid slip [8]. If however we assume that a no slip solid surface is covered with nanobubbles, the vertical viscous force is given by

$$F = -\frac{6\pi\eta a^2}{D} \left(V_S - \frac{dh}{dt} \right) \quad (2)$$

where V_S is the sphere velocity $V_S = d\omega \cos(\omega t)$ and h an average bubble thickness on the surface ¹. Hence, a time dependent mean bubble size $h(t)$ gives a natural way of modifying the viscous force. Indeed, we will show in what follows that small pressure fluctuations in the fluid gap lead to a first-order linear relation between the rate of change of the mean bubble height and the viscous force, $\dot{h} = -(k_1 F + k_2 \dot{F})$, where k_1 and k_2 are positive and shear-dependent. Equation (2) thereby leads to an effective $f^* < 1$:

$$f^* = \frac{1}{1 + \frac{6\pi\eta a^2 k_1}{D} + \left(\frac{6\pi\eta a^2 \omega k_2}{D}\right)^2 \left(1 + \frac{6\pi\eta a^2 k_1}{D}\right)^{-1}}. \quad (3)$$

We present in what follows a model leading to the values of (k_1, k_2) , and then compare to the Zhu & Granick experiments.

1 Setup and Nanobubble Stability

We need to study the response of nanobubbles to an oscillating pressure in the fluid. We suppose that a number density n of identical gas nanobubbles cover the bottom surface (in Figure 1), undeformed by viscous stresses ², and take h to be the average bubble thickness.

To perform the calculation, it is necessary to have a model for nanobubbles that is stable against dissolution. Diffusive equilibrium requires that the concentration of gas at the bubble surface equals the concentration c_∞ of gas dissolved in the liquid. Henry's law then implies that $p_{eq} = p_0 c_\infty / c_0$, where p_{eq} (p_0) is the equilibrium pressure in the bubble (liquid), and c_0 is the dissolved (saturated) gas concentration. The difficulty with nanobubble stability is that according to the ordinary Laplace law, $p_{eq} - p_0 = 2\gamma / R_0$, where γ is the liquid-gas surface tension and R_0 the radius of curvature of the bubble. Thus force equilibrium is inconsistent with diffusive stability [34]! The only possible explanation for experimental reports of stable nanobubbles existence is that the Laplace law is violated on these lengths scales. This is very natural, since surface tension arises from van der Waals forces, and in particular the influence of the solid surface has a range ~ 10 nm; one would expect that van der Waals interactions between the bubble surface and the solid are therefore important.

We therefore propose the following model for nanobubble stability: we modify the Laplace law by

$$p_{eq} - p_0 = \frac{2\gamma}{R_0} - f_\theta(R_0). \quad (4)$$

Here f_θ is a phenomenological function taking into account the forces that stabilize the bubble (θ is the liquid-solid contact angle). The only constraint on f_θ is that $R_0 f_\theta(R_0) \rightarrow 0$ as $R_0 \rightarrow \infty$, so the Laplace law is recovered in the macroscopic limit. For appropriate choice of f_θ , equation (4) models a candidate resolution to the nanobubble stability problem. In what follows, we assume that the function f_θ is of the form $f_\theta(R_0) = A(\theta) / R_0^\alpha$. The choice $\alpha = 2$ corresponds to the leading correction to the Laplace equation in terms of the interfacial curvature; it is similar to a Tolman's length-like modification of the surface tension [35, 36, 37], but due here to the influence of the solid

¹Equation (2) is valid assuming no-slip on the surface at $z = h(t)$; as was shown in [3, 2], even if the boundary condition on a bubble surface is that of no tangential stress, a continuous distribution of bubbles on a solid surface effectively produces no-slip because of the curvature of their interface, which justifies the assumption.

²This is equivalent as requiring a bubble Capillary number much smaller than unity; since the viscous stresses in the liquid increase with sphere radius a and fluid viscosity η , this limits therefore the range of η and a considered by the model.

surface and therefore much longer ranged. We emphasize however that a microscopic model might well lead to a more general f_θ , depending explicitly for example on the height of the bubbles, which shape as a result will not be spherical. Given the current knowledge of nanobubbles, we will consider however in this paper a simplified description and we will assume for simplicity that f_θ is only a function of the bubble radius. By doing so, we assume that the nanobubble shape is spherical. If $V = V(\theta)R^3$ is the volume of a single bubble, then the average thickness of the gas layer is $h(t) = nV(\theta)R(t)^3$. For spherical bubbles, we have $V(\theta) = \pi(1 - \cos\theta)^2(2 + \cos\theta)/3$.

2 Gas compression

Now we study the response of the bubbles to an external force F between the plates; this changes the liquid pressure from p_0 to p , and the pressure in the bubbles from p_{eq} to p_b . Here, S is the typical value of the sphere surface on which the viscous force acts $S = \pi L^2$ and L the radial geometrical length scale $L = (aD)^{1/2}$. At the small frequencies typical of squeeze flow experiments (1-10² Hz), the gas is isothermal, so the pressure in the bubble changes via the ideal gas law $p_b R^3 = p_{eq} R_0^3$. For small oscillations, the radius change is therefore $R - R_0 = R_0(p_{eq} - p_b)/3p_{eq}$.

In order for this radius change to be related to the applied force F we need to relate the change in bubble pressure to that in the liquid. Combining a perturbation of (4) around equilibrium with Henry's law and the ideal gas law leads to the relation between the dimensionless increases in pressure in both the bubble and the bulk

$$\frac{p_b - p_{eq}}{p_{eq}} = \beta \left(\frac{p - p_0}{p_0} \right) \quad (5)$$

where

$$\beta^{-1} = \left\{ \frac{c_\infty}{c_0} \left(1 - \frac{\alpha}{3} \right) + \frac{\alpha}{3} + \frac{2\gamma(\alpha - 1)}{3R_0 p_0} \right\}. \quad (6)$$

It is easily verified that β is always positive, so that a pressure change in the bubble is positively correlated with that in the bulk.

The viscous force on the sphere can now be directly related to the change in radius. Combining $F \approx (p - p_0)S$ with the ideal gas law and (5), we obtain $R \approx R_0(1 - \beta F/p_0 S)$; hence using $h = nV(\theta)R^3$, the rate of change of the mean bubble height h is given by

$$\frac{dh}{dt} \approx \frac{dh_0}{dt} - \left(\frac{3\beta h_0}{p_0 S} \right) \frac{dF}{dt}, \quad (7)$$

where h_0 is the average height of the unforced bubble. We thus have that the rate of change of the mean bubble height is the sum of the rate of change of the mean equilibrium bubble height h_0 , governed by gas diffusion, plus the second contribution due to the gas compressibility.

3 Gas diffusion

We now consider the rate of gas diffusion from the bubble. In our model for the oscillatory squeeze flow experiments [6, 8, 4, 12], bubbles lose mass by both vertical diffusion across the liquid layer and radial diffusion along the apparatus; because of the scale separation $D \ll a$, these two processes require separate treatment.

Let us first consider the case of vertical diffusion. Since for most common gases, $\kappa = \mathcal{O}(10^{-9})$ m²/s, the vertical oscillatory Peclet number, $Pe_v = D^2\omega/\kappa$, is always smaller than unity in the reported experiments: on the experimental time scale ω^{-1} , the bubbles are approximately in instantaneous vertical diffusive equilibrium. The

dissolved gas concentration above the bubble is therefore uniform throughout the liquid gap and is given, in the case of small amplitude oscillations, by Henry's law $c = p_b c_\infty / p_{eq}$. The number of gas molecules N per unit area necessary to fill the liquid gap at this concentration is equal to the gap thickness $(D - h_0)$ times the change in concentration $c_\infty(p_b/p_{eq} - 1)$. Using (5) we get that N is proportional to the viscous force

$$N = \frac{\beta c_\infty (D - h_0)}{\rho_0 S} F. \quad (8)$$

Since by definition, the instantaneous number of gas molecules per unit area is equal to $c_\infty \rho_0 h_0 / c_0$, the rate of change of h_0 is given by

$$\frac{dh_0}{dt} = \frac{dh_{0r}}{dt} - \frac{c_0}{c_\infty \rho_0} \frac{dN}{dt} = \frac{dh_{0r}}{dt} - \frac{\beta c_0 (D - h_0)}{\rho_0 p_0 S} \frac{dF}{dt} \quad (9)$$

where dh_{0r}/dt is the rate of change in the mean bubble height governed by gas diffusion in the (slowly varying) radial direction of the apparatus; let us now evaluate this contribution.

In contrast to the vertical case, the radial oscillatory Peclet number, $Pe_r = L^2 \omega / \kappa = a D \omega / \kappa$, is of order unity or larger, so that radial diffusion has to be accounted for explicitly. Assuming the dissolved gas is in vertical diffusive equilibrium, the equation for the time evolution of the mass of a gas bubble dm/dt is given by a flux integral on the bubble surface S_b

$$\frac{dm}{dt} = \kappa \int_{S_b} \mathbf{n} \cdot \nabla c \, dS = \kappa R^2 I(\theta) \frac{\partial c}{\partial r}, \quad (10)$$

where assuming a spherical bubble implies $I(\theta) = \pi(2(\pi - \theta) + \sin 2\theta)/2$. Further, the radial concentration gradient can be approximated by a simple linear law $\partial c / \partial r \approx (c_\infty - c) / L_r$ where $L_r \approx (\kappa / \omega)^{1/2} \approx L / Pe_r^{1/2}$ is the typical (shear dependent) radial gradient length scale³. When evaluating the bubble mass at the equilibrium pressure p_{eq} , $m = V(\theta) R_0^3 \rho_0 c_\infty / c_0 = h_0 \rho_0 c_\infty / c_0 n$, equation (10) together with Henry's law leads to a linear relation between the rate of change of h_{0r} and the viscous force

$$\frac{dh_{0r}}{dt} = - \frac{\kappa R_0^2 I(\theta) n c_0 \beta}{\rho_0 p_0 S L_r} F. \quad (11)$$

4 Final formula for f^*

With (7), (9) and (11), we obtain the final formula for f^* as (3), where (k_1, k_2) are given by

$$k_1 = \frac{n \kappa R_0^2 I(\theta) c_0 \beta}{\rho_0 p_0 S L_r}, \quad k_2 = \frac{3 \beta h_0 \rho_0 + \beta c_0 (D - h_0)}{\rho_0 p_0 S}. \quad (12)$$

In all cases, $f^* < 1$ and depends on both the gap thickness and the oscillation frequency.

5 Comparison with experiments

A comparison of the model with the experimental results of Zhu & Granick [8] is given in Figure 2 in the case of deionized water. We assume that the liquid was saturated with O₂ at 25°C and 1 atm ($\rho_0 = 1.28 \text{ kg/m}^3$, $c_0 = 8.3 \cdot 10^{-3} \text{ kg/m}^3$, $\kappa = 2 \cdot 10^{-9} \text{ m}^2/\text{s}$) and we take f_θ to be a power law with $\alpha = 2$; moreover, because both surfaces used in

³In general, the radial concentration of dissolved gas $c(r, t)$ verifies an advection-diffusion equation with shear dependent diffusivity [38]; however, for the small amplitude oscillation in [8], both advection and Taylor dispersion are negligible, and $c(r, t)$ satisfies a pure diffusion equation.

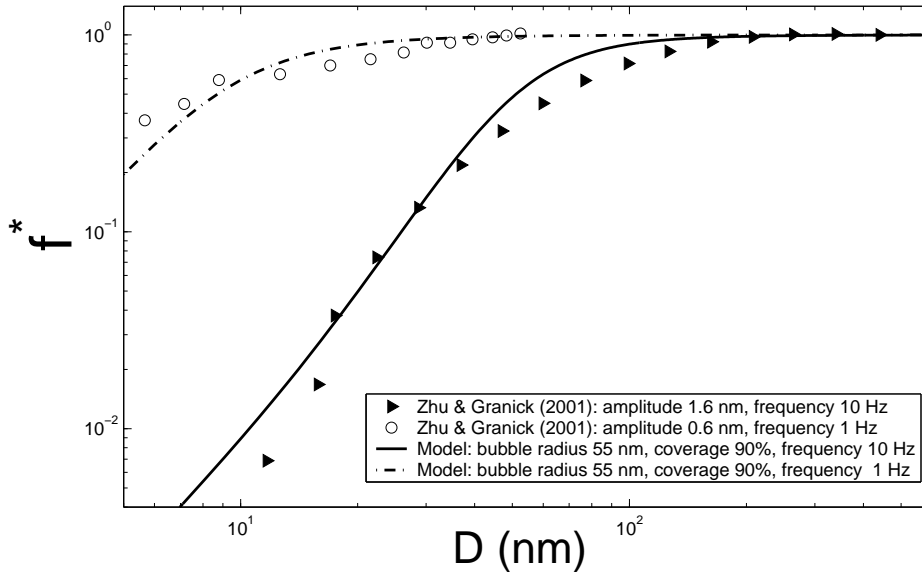


Figure 2: Comparison of the model with the small amplitude results of Zhu & Granick (2001) in the case of deionized water ($\theta = 110^\circ$): 90% of the surface is assumed to be covered with bubbles of radius $R_0 = 55$ nm and both 1Hz and 10Hz results are fitted by the model. The large amplitude results of Zhu & Granick (2001) can also be fitted by the model but are not reproduced here because, since the model assumes small amplitude oscillations, the fit would seem rather artificial.

[8] are hydrophobic, the values of k_1 and k_2 in (12) have to be multiplied by 2 in order to account for the rate of change of the bubble sizes on both surfaces. The small amplitude experimental data are found to be well predicted by the model (3) with a coverage of the surface with bubbles of 90%, similar to the high percentage observed in [21, 22], and a bubble radius of $R_0 = 55$ nm, in good agreement with the bubble sizes $R_0 \sim 100$ nm obtained by AFM measurements in [21, 22]. In all cases, the contribution to the decrease in f^* due to vertical diffusion is negligible; when $\omega = 10$ Hz, most (approximately 80%) of the decrease in f^* is due to compression; when $\omega = 1$ Hz, compression and radial diffusion are comparable

6 Discussion

We have shown that the time-dynamics of nanobubbles always leads to a decrease in the measured viscous force by a “leaking mattress” effect: as the solid sphere oscillates, periodic bubble compression and diffusion reduces the amount of liquid necessary to be squeezed out of the gap and thereby the viscous force. We emphasize that this mechanism is of *dynamic* origin, and is not a consequence of the microscopic slip at the bubble surfaces; in particular, we argue that this is why shear-dependent slip length have not been reported by investigations of slip in pressure-driven flow experiments [39, 40, 41, 10, 11, 18], where no oscillatory pressure is present to trigger an effect similar to the one presented here. Our linear model is based on two unknown parameters: the deviation from the Laplace law f_θ due to intermolecular forces, and the surface coverage of the bubbles, which might not be a surface property but could depend on the experimental procedure used to prepare the surfaces [20, 21, 22]. Additional contributions

to (k_1, k_2) could come from bridging bubbles (which, even though they are not considered in the present model, are not ruled out by the measurements reported in [8] which report peak forces only)), large amplitude oscillations and displacement of the bubbles on the solid surface. We note finally that the apparent slip we obtain increases with the fluid viscosity, in agreement with experiments [7, 10]; it also increases with the size of the sphere a , which might account for the large slip lengths reported in [8] (cm-size spheres) as opposed to other squeeze flow experiments (usually μm -size spheres). The apparent slip length is therefore not only a solid/liquid property but depends on the system size [18]. Finally, we note that increasing surface roughness will destroy the leaking mattress effect: once the scale of the roughness is of order that of the bubbles, the dynamics described here no longer applies.

Acknowledgments

We are grateful to Jacquie Ashmore, Todd Squires, José Gordillo, Howard Stone and Steve Granick for useful discussions. We also thank Steve Granick for useful information about Figure 2 in the paper [8]. This research was supported by the Harvard MRSEC, and the NSF Division of Mathematical Sciences.

References

- [1] Goldstein S. (1938) *Modern Developments in Fluid Dynamics*, vol. II, 676-680 (Clarendon Press).
- [2] Richardson, S. (1973) *J. Fluid Mech.* **59**, 707-719.
- [3] Jansons, K.M. (1988) *Phys. Fluids* **31**, 15-17.
- [4] Zhu, X. and Granick, S. (2002) *Phys. Rev. Lett.* **88**, 106102.
- [5] Pit, R., Hervert, H. and Léger, L. (2000) *Phys. Rev. Lett.* **85**, 980-983.
- [6] Baudry, J. and Charlaix, E. (2001) *Langmuir* **17**, 5232-5236.
- [7] Craig, V.S.J., Neto, C. and Williams, D.R.M. (2001) *Phys. Rev. Lett.* **87**, 054504.
- [8] Zhu, X. and Granick, S. (2001) *Phys. Rev. Lett.* **87**, 096105.
- [9] Bonaccorso, E., Kappl, M. and Butt, H.-S. (2002) *Phys. Rev. Lett.* **88**, 076103.
- [10] Cheng, J.-T. and Giordano, N. (2002) *Phys. Rev. E* **65**, 031206.
- [11] Tretheway, D.C. and Meinhart, C.D. (2002) *Phys. Fluids* **14**, L9-L12.
- [12] Cottin-Bizonne, C., Jurine, S., Baudry, J., Crassous, J., Restagno, F. and Charlaix, E. (2002) Submitted to *Eur. Phys. J.*
- [13] Thompson, P.A. and Troian, S.M. (1997) *Nature* **389**, 360-362.
- [14] Barrat, J.-L. and Bocquet, L. (1999) *Phys. Rev. Lett.* **82**, 4671-4674.
- [15] Brenner, H. and Ganesan, V. (2000) *Phys. Rev. E* **61**, 6879.

- [16] Cieplak, M., Koplik, J. and Banavar, J.R. (2001) *Phys. Rev. Lett.* **86**, 803-806.
- [17] Denniston, C. and Robbins, M.O. (2001) *Phys. Rev. Lett.* **87**, 178302.
- [18] Lauga, E. and Stone, H.A. (2002) Submitted to *J. Fluid Mech.*
- [19] Navier, C.L.M.H. (1823) *Mémoires de l'Académie Royale des Sciences de l'Institut de France* **VI**, 389-440.
- [20] Ishida, N., Inoue, T., Miyahara, M. and Higashitani, K. (2000) *Langmuir* **16**, 6377-6380.
- [21] Tyrrell, J.W.G. and Attard, P. (2001) *Phys. Rev. Lett.* **87**, 176104.
- [22] Tyrrell, J.W.G. and Attard, P. (2002) *Langmuir* **18**, 160-167.
- [23] Parker, J.L., Claesson, P.M. and Attard, P. (1994) *J. Phys. Chem.* **98**, 8468-8480.
- [24] Carambassis, A., Jonker, L.C., Attard, P. and Rutland, M.W. (1998) *Phys. Rev. Lett.* **80**, 5357-5360.
- [25] Mahnke, J., Stearnes, J., Hayes, R.A., Fornasiero, D. and Ralston, J. (1999) *Phys. Chem. Chem. Phys.* **1**, 2793-2798.
- [26] Attard, P. (2000) *Langmuir* **16**, 4455-4466.
- [27] Ishida, N., Sakamoto, M., Miyahara, M. and Higashitani, K. (2000a) *Langmuir* **16**, 5681-5687.
- [28] Yakubov, G.E., Butt, H.-S. and Vinogradova, O.I. (2000) *J. Phys. Chem. B* **104**, 3407-3410.
- [29] Attard, P., Moody, M.P. and Tyrrell, J.W.G. (2002) *Physica A* **314**, 696-705.
- [30] Ishida, N., Sakamoto, M., Miyahara, M. and Higashitani, K. (2002) *J. Colloid Interf. Sci.* **253**, 112-116.
- [31] Sakamoto, M., Kanda, Y., Miyahara, M. and Higashitani, K. (2002) *Langmuir* **18**, 5713-5719.
- [32] de Gennes P.G. (2002) *Langmuir* **18**, 3413-3414.
- [33] Vinogradova, O.I. (1995) *Langmuir* **11**, 2213-2220.
- [34] Ljunggren S. and Eriksson J.C. (1997) *Colloids Surf. A* **129-130**, 151-155.
- [35] Tolman, R.C. (1949) *J. Chem. Phys.* **17**, 333.
- [36] Thompson, S.M., Gubbins, K.E., Walton, J.P.R.B., Chantry, R.A.R. and Rowlinson, J.S. (1984) *J. Chem. Phys.* **81**, 530-.
- [37] Blokhuis, E.M. and Bedeaux, D. (1992) *J. Chem. Phys.* **97**, 3576-3586.
- [38] Taylor, G.I. (1953) *Proc. Roy. Soc. A* **219**, 186-203.
- [39] Schnell, E. (1956) *J. Appl. Phys.* **27**, 1149-1152.
- [40] Churaev, N.V., Sobolev, V.D. & Somov, A.N. (1984) *J. Colloid. Int. Sci.* **97**, 574-581.
- [41] Watanabe, K., Udagawa, Y., & Udagawa, H. (1999) *J. Fluid Mech.* **381**, 225-238.